

Measuring the Root Length of Peanuts Grown in Rhizotrons Using Computer Vision

Leonardo Michalski Stefanello*, Leonardo Paillo da Silva*, Luís Henrique Soares Dayrell*,
Jayme Ferrari Neto*, Hemerson Pistori*[†], Higor Henrique Picoli Nucci[†]

*Universidade Católica Dom Bosco

Av. Tamandaré, 6000 CEP 79117-900, Campo Grande, MS, Brazil

[†]Universidade Federal do Mato Grosso do Sul

Av. Costa e Silva, s/n^o – Bairro Universitário, CEP 79070-900, Campo Grande, MS, Brazil

Email: msleonardo.1998@gmail.com, leopaillo2005@gmail.com,

luishkorocg@hotmail.com, rf3513@ucdb.br, pistori@ucdb.br, higorrucci@gmail.com

Abstract—Peanut is one of the most grown leguminous crops in the world, but it can suffer during water deficit periods. In this paper, a new method to help monitoring root growth for laboratory experiments with this plant is proposed. By using a new combination of smoothing, thresholding, morphological filtering and skeletonization, our method has achieved a correlation of 0.968 with the Tennant’s standard approach.

I. INTRODUCTION

The peanut (*Arachis hypogaea* L.) is a leguminous plant originally from South America but that is commonly cultivated in countries with a warm climate from Asia, Africa and the Americas. It is a product consumed worldwide and has as some of its purposes the production of vegetable oil and animal feed. Among the legumes, peanuts are one of the main crops, with China being a major producer with an output reaching 17.33m in 2019 [1].

The inoculation of peanut seeds with bacteria, as for instance the *Azospirillum brasiliense*, can promote greater root growth, thus giving a higher tolerance to periods of water deficit. Inoculation with such bacteria can also result in higher plant height and more mass [2]. In order to measure a plant’s root growth an equipment called rhizotron is usually used [3, 4, 5]. The rhizotron used in our experiments, shown in Figure 1, is made of PVC tubes, with a diameter of 0.20m and a height of 1.00m. The tubes were cut in half in the longitudinal direction, forming a flat face, where a glass wall was installed.

In the traditional Tennant’s method to measure the root length, a drawing of the root is made using a transparent plastic sheet that is then put over a grid paper. Each cell of the grid that intersects the root is counted and a conversion considering the cell size is used to produce an estimation for the root total length. In this paper, a new method to turn this process less time-consuming and prone to errors is proposed by using a smartphone to photograph the transparent plastic sheet and one software that uses computer vision to automatically calculate the root length. The computer vision software is a novel combination of several filters, skeletonization and graph based line length estimator. Bar graphs and regression lines are used



Fig. 1: Rhizotron inside a green house showing the roots of 3 peanut plants used in our experiments

to investigate the proposed approach performance. The results showed a high correlation between the proposed approach and the traditional one.

II. MATERIALS AND METHODS

The proposed approach to calculate the peanut roots length is a sequence of image processing steps. The input is a photo from the transparent plastic sheet where the roots were drawn by hand, following the contour of the actual root. In order to provide a higher contrast between the root drawing and the background, the transparent plastic sheet is put over a white matt paper, as shown in Figure 2a. Then the image captured is manually cropped to remove elements that are not related to the problem at hand. Some image editing is

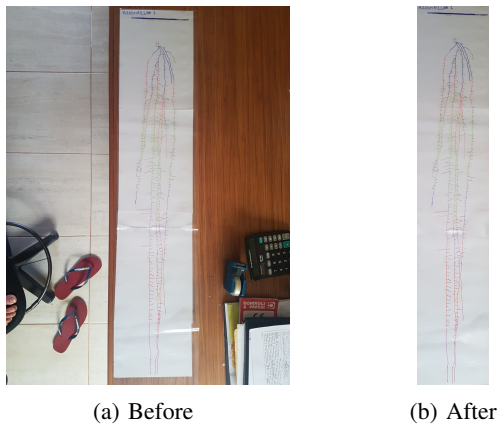


Fig. 2: Root drawing image preparation before the automatic length measuring: (a) original image and (b) image after cropping and edition in order to remove false lines

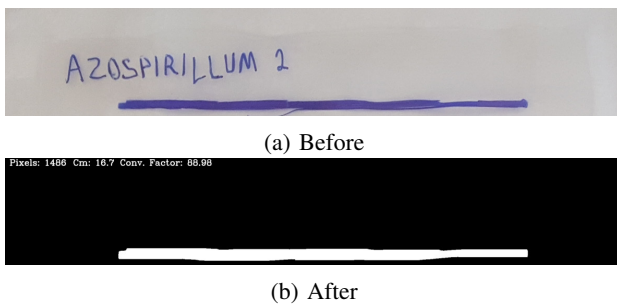


Fig. 3: Image top region where the calibration line is drawn before (a) and after (b) image processing and conversion factor calculation. In this example, the line has 1486 pixels and 16.7 cm, given a conversion factor of 88.98

sometimes necessary to remove the false lines introduced by light reflections and paper or plastic disruptions. The result of the cropping and editing operation is exemplified in Figure 2b.

The first image processing step automatically crops the upper part of the image containing a thick calibration line with a known length, around 17cm (see Figure 3). The length of this line is measured in pixels, by the software, and a conversion formula is derived to provide an output in centimeters. The agronomic treatment name that appears above the calibration line is removed using a morphological opening operation with a horizontal line structuring element (3x200 pixels in size). Figures 3a and 3b show the calibration line before and after the image processing step that calculates the conversion factor between pixels and centimeters.

After calibration, the image is cropped again to contain only the root and is converted to gray scale and smoothed using a bilateral filter [6], which is a non-linear filter that aims to reduce noise without blurring the edges. The bilateral filter has two important parameters, sigmaColor (SC) and sigmaSpace (SS), that control how the color range distance and space distance between two pixels will affect the smoothing results, respectively. The proposed approach does not use color

information like in the manual method because we assume that new images will be captured at each growing stage of the plant. The color range distance in this case is related to the pixel gray value after color to gray scale conversion. The best values for these and other parameters are found using a subset of all the images collected during the experiment, in a process called parameter-tuning.

The smoothed image is then binarized using a local approach called adaptive Gaussian threshold [7] that has two parameters: a block size (BS) that controls the size of the area around each pixels that will be used to calculate that binarization threshold; and the C parameter that is subtracted from the weighted mean values around a pixel and is used to decide if this pixel will be changed to black or to white. After binarization, the images are processed using the opening and closing morphological operators to filter out small artifacts that are not linked to the root and to close gaps that may appear in the root image during processing or image capture. These operators are controlled by a parameter linked to the size of the structuring element, in our case, a square. We have tested different sizes for opening (OS) and closing (CS) during parameter-tuning.

The last image processing step is called skeletonization and it produces an image of the root with thin lines that are all only one pixel large. This is a very important step that enables the length calculation in pixels, that are then converted to centimeters using the conversion factor calculated in the first step. The skeletonization is made using the algorithm proposed by Zhang and Suen [8] that works by successively removing one pixel from the objects borders. Figure 4 shows the original image, the gray scale smoothed version and the final skeleton. At the bottom of the third image the lengths calculated using the manual method (314.679) and the automated one (306.92) are shown, in centimeters. The difference between the manual and automated methods is also shown in brackets (2.78%).

All the image processing steps described so far have been implemented using the numpy, opencv [9] and scikit-image [10] packages. The skeleton length calculation was made using the skan package [11] that uses a graph based approach to represent the adjacency relations between the skeleton pixels. In this way, the algorithm can distinguish between junctions, end points and internal paths to estimate the length of all skeletons branches. A final parameter, the minimum length (ML), was introduced in our proposal to be used as a threshold to cut from the final length small objects that are not part of the root but was not removed during the previous steps. All objects with lengths smaller than ML are discarded from the final length computation.

The parameter tuning was made using 50% of the images available (training set) and the other 50% (test set) have been used to estimate the proposed approach performance using the mean absolute error (MAE) and the mean absolute percentage errors (MAPE) metric. The Pearson's correlation coefficient (r) between the manual and the automatic length measures has also been calculated for the test set. During parameter tuning, the best value for the seven parameters was calculated



Fig. 4: Sequence showing (a) the Original image, (b) the image after gray scale conversion and smoothing and (c) the image skeleton with final measurement results at the bottom

independently for (1) SC and SS; (2) BS and C; (3) OS and CS and (4) ML. Table II summarizes these parameters, showing the set of values used during tuning. The values follow a geometric progression as it would be computationally infeasible to test all possible combinations. The percentile difference between manual and automatic measurements has been chosen as the main performance metric and the best value for each parameter has been chosen by comparing the median values for this metric over the training set.

TABLE I: Set of values used for each parameter of the proposed approach during tuning

Param.	Description	Tested Values
SC	Sigma Color	10 20 40 80 160
SS	Sigma Space	1 2 4 8 16 32
BS	Block Size	3 7 15 31 63 127 255
C	C	2 4 8 16
OS	Opening Size	2 4 8 16
CS	Closing Size	2 4 8 16
ML	Minimum Length	0 10 20 40 80

The dataset is composed of images taken during an agronomic experiment with peanut plants that happened between April 9 and May 21, 2020, inside a green house in the Dom Bosco Catholic University campus, Campo Grande, Brazil. A total of 24 peanut seeds have been planted in 24 rhizotrons and the Tennant's method [12] has been used to measure the root

TABLE II: Best values chosen using the parameters tuning boxplots

Param.	Description	Best Value
SC	Sigma Color	20
SS	Sigma Space	2
BS	Block Size	15
C	C	2
OS	Opening Size	2
CS	Closing Size	4
ML	Minimum Length	10

growth two times a week: days 7, 11, 14, 18, 21, 25, 28, 32, 35 and 39 after planting. In some of these days, pictures have been taken from some of the transparent plastic sheets used in the Tennant's method, giving a total of 30 images, 15 (50%) were used for training (parameter tuning) and 15 (50%) for testing the proposed approach. Figure 8 shows four examples of images from this dataset corresponding to different days and treatments. Figures 5a and 5b are from the same plant treated with azospirillum in days 14 and 28. Figures 5c and 5d are from two different control plants in days 11 and 25. The images were taken using a smartphone model.

III. RESULTS

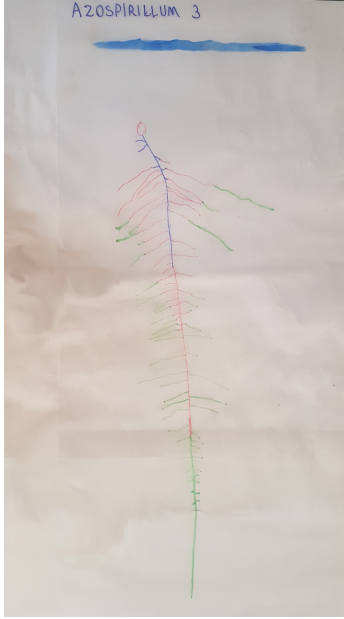
Table II shows the best values for all the hyperparameters that have been selected using the training dataset and then set as the default values to test the proposed approach on the test set. The bar graphs in Figure 6a compare the references (Tennant's) lengths and the lengths calculated using our proposed approach on the training set, while Figure 6b compares the same two strategies, Tennant's and ours, using the test dataset.

It is evident from the bar graphs in Figure 6 that for most of the images our methods compares well to the Tennant's approach, both in the training and test set. The Pearson correlation (r) on the test set was 0.968, which indicates a very high correlation that can be observed through the regression line and points drawn in Figure 7b. The mean absolute error (MAE) and the mean absolute percentage errors (MAPE) were, respectively, 44.4 and 22.9, indicating that in spite of the high correlation, there is some room for improvements.

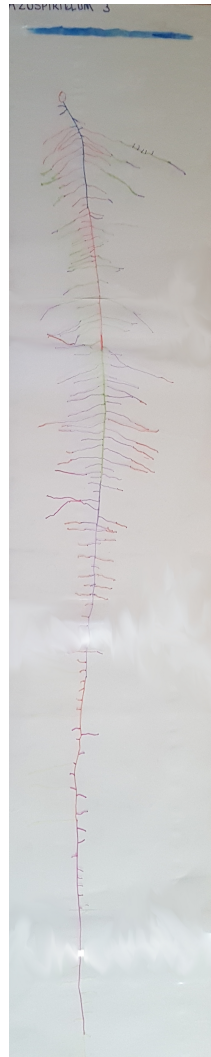
Table III shows, for each image from the test set, the absolute and percentage difference between our method and the standard. There is a clear outlier, image T1-A-6, with a percentage error greater than 50% (52.74%) that has a great impact on MAE and MAPE. The best results, for the A6-D-5 image, the system achieved an error of just 2.84%.

IV. DISCUSSION

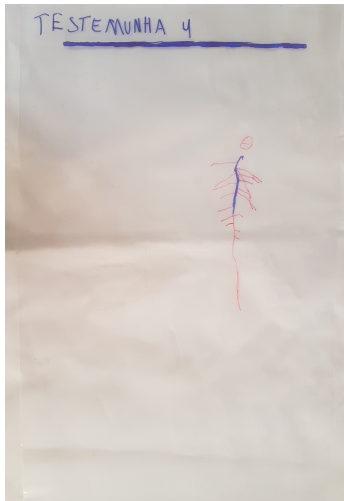
The proposed automated root measuring method, as aforementioned, was intended to be less time-consuming and prone to errors when compared to other automated and manual methods. Moreover, the Pearson correlation between the proposed approach and Tennant's manual method was 0.968, showing that our procedure was proven to be highly accurate. With that in mind, it is essential to review our experiments and find room



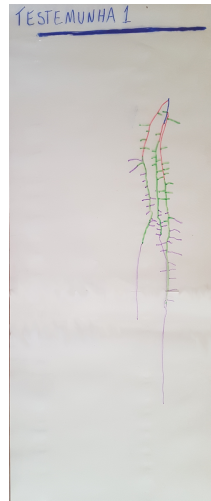
(a) Azospirillum, day 14



(b) Azospirillum, day 28

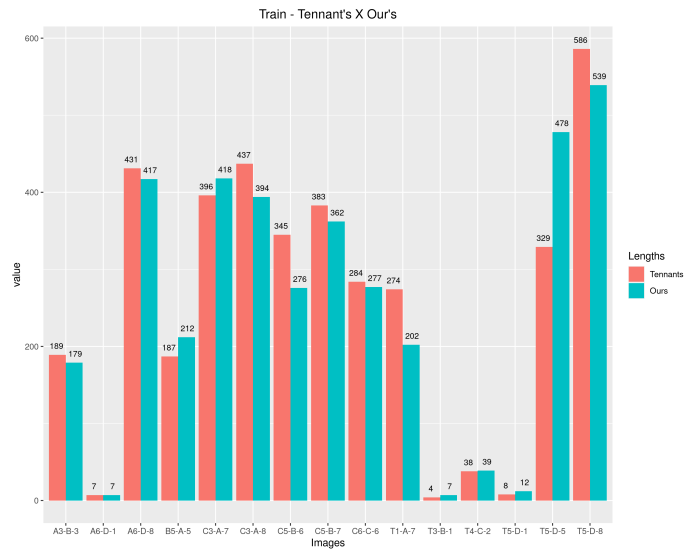


(c) Control, day 11

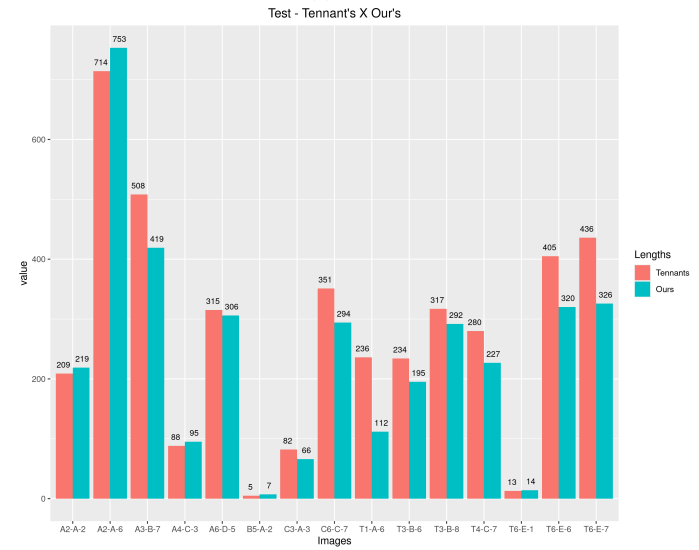


(d) Another control, day 25

Fig. 5: Some examples of the images that compose the dataset used in the experiments. The roots are in different growth stages



(a) Train

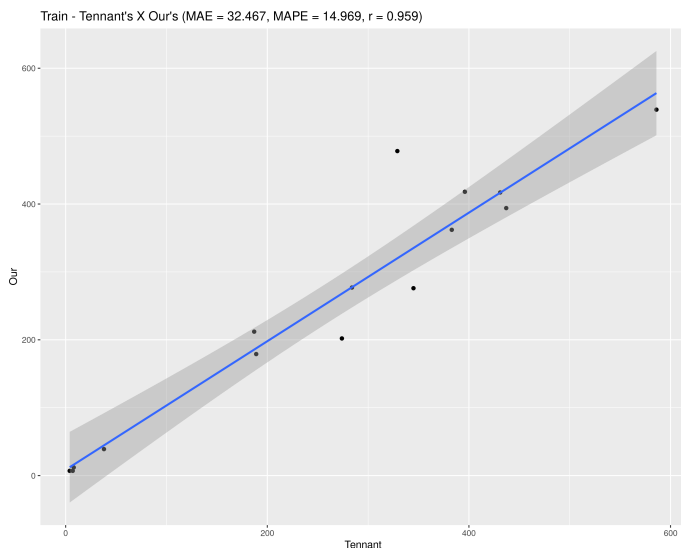


(b) Test

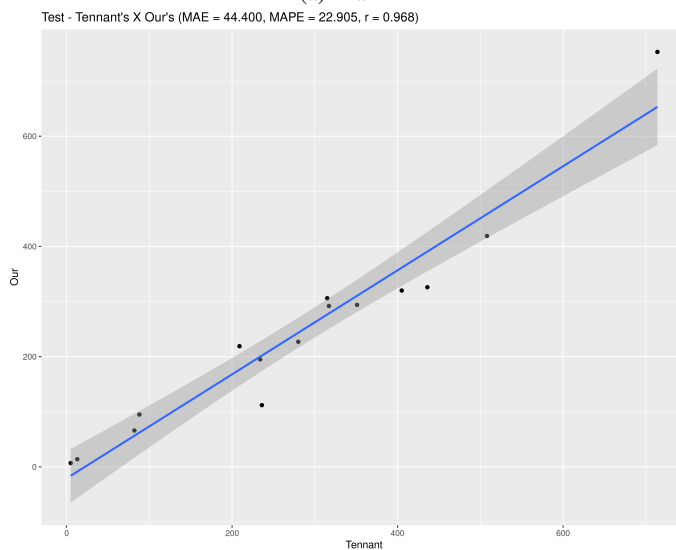
Fig. 6: Bar graph showing the manual (Tennant's) and automatic (our's) lengths over the images from the (a) training and the (b) test set.

for future improvements, while also highlighting its positive features when compared to related researches and studies.

For instance, Dong et al. [13] have developed a method that consists in coupling a notebook and a flatbed scanner to a rhizotron containing *Malus domestica* roots, in order to obtain high-resolution root images and then estimate their lengths by using a computer image analysis system. For the purpose of obtaining the images, the door blocking the rhizotron's transparent wall should be opened, so that the researchers could press the scanner to the box. This simple and practical automatized technique allowed the researchers to monitor numerous and relatively large roots frequently, while getting a notable correlation of ($r=0.75$) with Tennant's method.



(a) Train



(b) Test

Fig. 7: Scatter plot with regression bar for manual (Tennant's) against automatic (our's) lengths over the images from the (a) training and the (b) test set.

When compared to this scanning method, our approach is generally simpler and more affordable, given that it only requires a few tools, like a phone or any other camera device. Moreover, it does not require any specific managements on distancing or lighting, since the aforementioned calibration line allows the computer to establish a conversion factor between the image's length in pixels and centimeters. However, our technique has faced a few limitations in the measuring process, mainly in its image processing step.

In order to address those limitations, the roots in which our method differed the most from the traditional method should be analyzed, especially the image T1-A-6, according to the Table III. This image, shown in Figure 8a, had as

TABLE III: Differences between the proposed approach and Tennant's ordered by the best to the worst case

Image	Tennant	Our	Dif.	Perc.Dif.
Image	Tennant	Our	Dif.	Perc.Dif.
A6-D-5	315	306	8.93	2.84%
A2-A-2	209	219	9.73	4.65%
A2-A-6	714	753	39.24	5.49%
A4-C-3	88	95	6.66	7.57%
T3-B-8	317	292	24.97	7.87%
T6-E-1	13	14	1.37	10.55%
C6-C-7	351	294	57.4	16.34%
T3-B-6	234	195	38.47	16.46%
A3-B-7	508	419	89.34	17.59%
T4-C-7	280	227	52.51	18.77%
C3-A-3	82	66	15.68	19.19%
T6-E-6	405	320	85.63	21.12%
T6-E-7	436	326	110.75	25.37%
B5-A-2	5	7	1.43	27.96%
T1-A-6	236	112	124.74	52.74%

an outcome in its automatic measurement a discrepancy of 52.74% from the manual measurement. By analyzing the drawn root's structure and how the software ran it, it's possible to infer that the greatest outlier in this case was the region where both green and purple drawn lines were very close to each other (Figures 8b and 8c). As a result, the software couldn't detect the two different lines and registered them as only one single line, as shown in Figure 8d, making the result substantially lower than the expected.

This is a case in which the parameters defined with the training set were not enough to measure this root correctly, most likely because there were little to no similar structures in the training set. Although the computer vision software in general was not designed for this kind of input, which aims for one-dimensional structures as an outcome, there are plenty of ways of improving those results in future experiments, mainly in the input itself. For instance, different kinds of pens or markers, preferably with thicker tips, could be used, in order to make each color stand out more. A less reflective material, like vegetal paper, could be used in the process of hand drawing and photography, making the images clearer. Lastly, the roots could be drawn in different paper layers, mainly in cases like this, so that different images generated and then and then overlaid during the skeletonization process. There can also be improvements in the software itself, mainly in the defined parameters, by making them more specific according to further testings. Furthermore, it's important to note that our method faces physical limitations, like the size of the rhizotrons and the root's two-dimensional view, which makes the technique unable to measure large roots or monocotyledon plants' roots. Thereafter, it is viable to state that our method is efficient for measuring smaller plant root lengths in a quick, automated way.

V. CONCLUSION

A new approach to aid in the process of plant root estimation has been proposed and tested. The results are encouraging and differently from most of the solutions currently available, the method does not require any special imaging equipment, just a

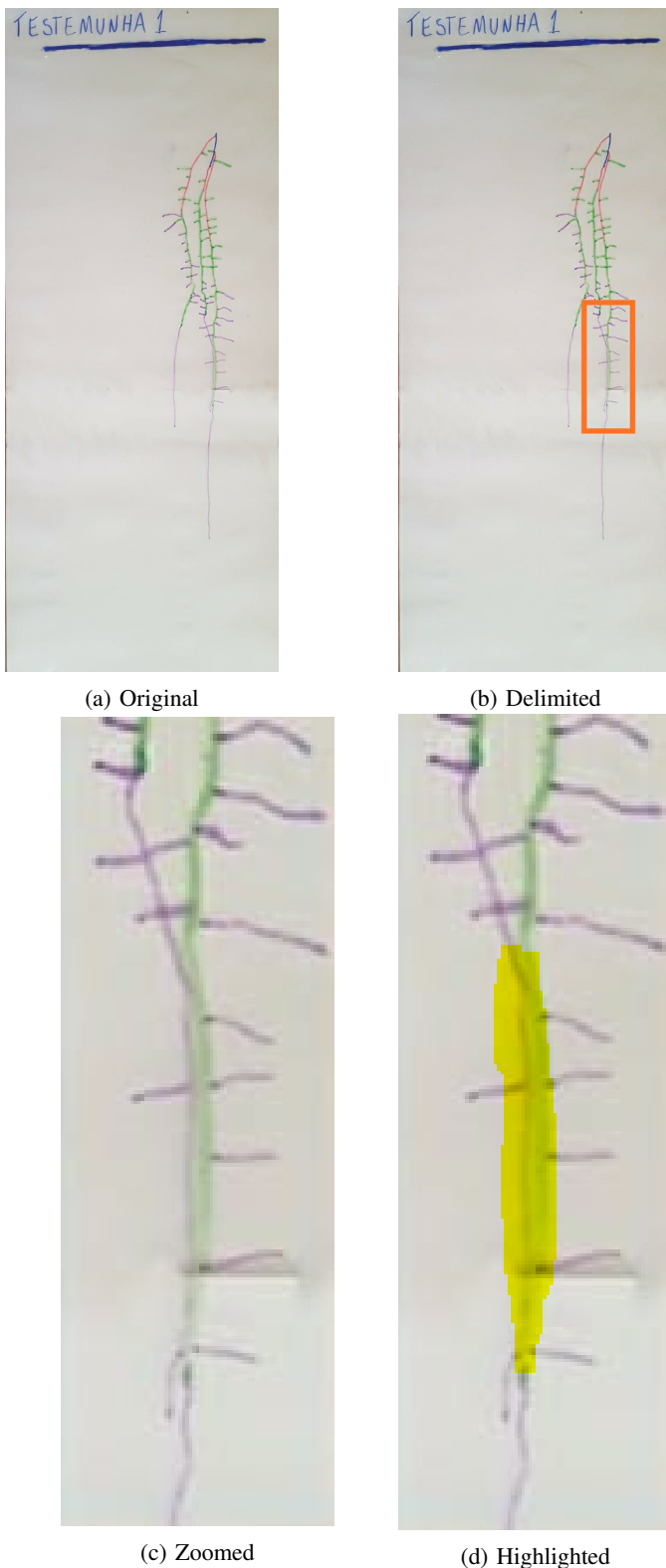


Fig. 8: Sequence that shows (a) the image T1-A-6, (b) the delimitation on the region where its length was miscalculated the most, (c) a close-up on the region and (d) a yellow highlight on its problematic portion

common cell phone. For future works, we envision optimizing our methods and the measurement procedures - for instance, by using an object of known length for calibration instead of a drawn line, raising the accuracy of the length conversion -, as well as testing the proposed approach directly on images from the rhizotron and not from the transparent plastic sheet, turning the method even more efficient and less time consuming.

ACKNOWLEDGMENT

This work has received financial support from the Dom Bosco Catholic University and the Foundation for the Support and Development of Education, Science and Technology from the State of Mato Grosso do Sul, FUNDECT. Some of the authors have been awarded with Scholarships from the the Brazilian National Council of Technological and Scientific Development, CNPq, and the Coordination for the Improvement of Higher Education Personnel, CAPES. We would also like to thank NVIDIA for providing the Titan X GPUs used in the experiments.

REFERENCES

- [1] L. Wang, Q. Yang, and H. Zhao, "Sub-regional identification of peanuts from shandong province of china based on fourier transform infrared (ft-ir) spectroscopy," *Food Control*, vol. 124, p. 107879, 2021.
- [2] G. d. S. Freitas, G. F. Barbosa, A. M. Zuffo, and F. Steiner, "Co-inoculation of peanut (*arachis hypogaea* l.) with bradyrhizobium and azospirillum promotes greater tolerance to drought," *Research, Society and Development*, vol. 9, no. 7, p. e69973690, Apr. 2020.
- [3] F. R. Echer, P. R. L. Zanfolin, A. C. M. Moreira, A. C. P. Santos, and P. H. Gorni, "Root growth and carbohydrate partitioning in cotton subjected to shading in the initial phase," *Ciência Rural*, vol. 49, no. 1, 2019.
- [4] M. Gidea, M. Magureanu, R. I. Teodorescu, L. M. Iosub, and D. Cimponeriu, "The impact of plasma treatment over wheat seeds," *International Multidisciplinary Scientific GeoConference: SGEM*, vol. 17, pp. 361–368, 2017.
- [5] J. M. Gandullo Tovar, S. Ahmad, E. Darwish, R. Karlova, and C. Testerink, "Phenotyping tomato root developmental plasticity in response to salinity in soil rhizotrons," *Plant Phenomics*, 2760532., 2021.
- [6] C. Tomasi and R. Manduchi, "Bilateral filtering for gray and color images," in *Sixth international conference on computer vision (IEEE Cat. No. 98CH36271)*. IEEE, 1998, pp. 839–846.
- [7] N. Khetan, L. Kejriwal, and S. Indu, "Enhancement of degraded manuscript images using adaptive gaussian thresholding," *International Journal of Future Generation Communication and Networking*, vol. 10, no. 1, pp. 47–60, 2017.
- [8] T. Zhang and C. Y. Suen, "A fast parallel algorithm for thinning digital patterns," *Communications of the ACM*, vol. 27, no. 3, pp. 236–239, 1984.
- [9] G. Bradski, "The OpenCV Library," *Dr. Dobb's Journal of Software Tools*, 2000.

- [10] S. van der Walt, J. L. Schönberger, J. Nunez-Iglesias, F. Boulogne, J. D. Warner, N. Yager, E. Gouillart, T. Yu, and the scikit-image contributors, “scikit-image: image processing in Python,” *PeerJ*, vol. 2, p. e453, 6 2014. [Online]. Available: <https://doi.org/10.7717/peerj.453>
- [11] J. Nunez-Iglesias, A. J. Blanch, O. Looker, M. W. Dixon, and L. Tilley, “A new python library to analyse skeleton images confirms malaria parasite remodelling of the red blood cell membrane skeleton,” *PeerJ*, vol. 6, pp. e4312–e4312, Feb 2018, 29472997[pmid], PMC5816961[pmcid], 4312[PII]. [Online]. Available: <https://pubmed.ncbi.nlm.nih.gov/29472997> , <https://doi.org/10.7717/peerj.4312>
- [12] D. Tennant, “A test of a modified line intersect method of estimating root length,” *The Journal of Ecology*, pp. 995–1001, 1975.
- [13] S. Dong, D. Neilsen, G. H. Neilsen, and M. Weis, “A scanner-based root image acquisition technique for measuring roots on a rhizotron window,” *HortScience*, vol. 38, pp. 1385–1388, 2003.